σ Octantis

Bill Rea
Richmond, New Zealand; rea.william@gmail.com

Received December 2, 2022; revised February 3, March 3, 2023; accepted March 15, 2023

Abstract We examine data from three Sectors of observations from NASA's Transiting Exoplanet Survey Satellite (TESS) for the δ Scuti star σ Octantis = HD 177482. We were unable to conclude that it is a hybrid δ Sct/γ Dor variable as reported in earlier literature because the evidence for the presence of active γ Dor frequencies was absent from one Sector's data and only weakly statistically significant in the other two. We report that several of the δ Sct frequencies showed statistically significant amplitude modulation between the three TESS Sectors.

1. Introduction

On the HR diagram the δ Scuti variables lie at the intersection of the main sequence and the classical instability strip. Diagrams showing the location of different types of pulsating variables, such as Figure 3.2 of Catelan and Smith (2015), often show the regions occupied by roAp, δ Sct, SX Phe, γ Dor, and RR Lyr variables overlapping to some extent. Of particular interest for asteroseismology are stars which lie in the overlapping regions of δ Sct and γ Doradus variables because these stars should pulsate in both pressure and gravity modes (p- and g-modes), which are the pulsation modes of δ Sct and γ Dor variables, respectively.

Although the prototype for the class, δ Sct, was known to be variable since Campbell and Wright (1900), as a class they were not recognized as a distinct group of variable stars until Eggen (1956). The discovery of the γ Dor class of variables is usually credited to Balona *et al.* (1994), but it is clear that they drew on evidence from a number of authors published over the previous 20 years and conference papers on them had appeared earlier such as Krisciunas (1993). However, it has also been known almost as long as they have been recognized as a separate class of pulsators that the two regions overlap so that a single star may pulsate with both δ Sct and γ Dor frequencies (Breger and Beichbuchner 1996). Such stars are known as hybrid δ Sct/γ Dor stars.

σ Octantis = HD 177482 (see Table 1 for some basic data) was first identified as a δ Sct by McInally and Austin (1978) based on observations obtained using the Optical Craftsmen 61-cm telescope at University of Canterbury's Mt. John Observatory and, apart from the paper of Crouzet *et al.* (2018), has been little studied since then. It was the subject of two very short papers by Coates *et al.* (1981) and Tsvetkov (1982) which did little more than establish a single pulsation period of 0.097 day together with its amplitude of $\Delta V = 0.025$ magnitudes and a conjecture that it pulsates only in the fundamental mode. The 848 observations in the American Association of Variable Star Observers International Database (AAVSO; Kafka 2022) were obtained in a few short observing sessions in 1981, 1986, and 1989. The 1981 observations contributed to Coates *et al.* (1981) but the later work, by the Auckland Photoelectric Observers Group, does not appear to have led to further analysis and publication.

Based on four Antarctic winter seasons of photometry from 2008 to 2011, Crouzet *et al.* (2018) recently reported that σ Oct was a hybrid δ Sct/γ Dor pulsator, and they reported 21 active frequencies, 17 within the δ Sct range and four within the γ Dor range. Crouzet *et al.* (2018) reported that four of the δ Sct frequencies showed amplitude modulation, confirming Bowman *et al.* (2016), who studied 983 δ Sct stars observed by *Kepler*, and reported that 61.3% exhibited amplitude modulation. In particular, the amplitude of σ Oct's main frequency of the first two seasons' observations (2008 and 2009), approximately 10.49 cycles d^{-1}, decreased by a factor of almost 10 during the final seasons of observations (2010 and 2011) meaning that it was no longer the highest amplitude frequency. They further reported that the γ Dor frequencies had low amplitudes.

The unpublished report of Rea (2019), based on 350 high resolution spectra from two, two-week observing runs, also concluded that σ Oct had both δ Sct and γ Dor pulsations active and hence should be considered a hybrid δ Sct/γ Dor variable.

This paper analyzes data from the Transiting Exoplanet Survey Satellite (TESS) (Ricker *et al.* 2014), which observed σ Oct in sectors 12, 27, and 39 of its mission. Table 2 gives the date ranges for the observations within these sectors. This provides a useful set of data to check the conclusions of these previous works and look for any changes in the active frequencies.

The remainder of the paper is structured as follows. section 2 gives details of the data used, section 3 presents the results of the frequency analyses carried out, section 4 contains the discussion, and section 5 gives our conclusions.

Table 1. Basic data on σ Oct.

Parameter	*Value*	*Source*
R.A.	$21^h\ 08^m\ 46.85^s$	VSX
Dec.	–88° 57' 23.4"	VSX
Spectral Type	F0IV	VSX/SIMBAD
Period	0.097 d/2.3 h	VSX
Magnitude	5.45 V	VSX
Amplitude	0.05 V	VSX
Distance	90.09 pc ± 0.50	Gaia
TIC	468184895	TASOC

Notes: TIC is the TESS Input Catalogue number. The sources are: the Variable Star Index (VSX; Watson et al. *2014); SIMBAD (CDS Strasbourg 2007); Gaia Collab. (2020), and TASOC (2023).*

2. Data and methods

2.1. Data

The raw data for this paper were downloaded from the TESS Asteroseismic Science Operations Center (TASOC; https://tasoc.dk). Sector 12 data were downloaded on 30 Jun 2020, Sector 27 data on 30 Nov 2020, and Sector 39 data on 19 May 2022.

The reported corrected flux was converted to magnitudes using the value for σ Oct's magnitude in the V band as reported on the TASOC web site as the mean value for each observation run. Observations were discarded if the value in the Pixel Quality Field (PQF) was non-zero or either the date or the corrected flux was recorded as not-a-number (nan). Table 2 summarizes the date ranges and number of usable data points for each sector's observations.

2.2. Frequency analysis

Frequency analysis was carried out using three software packages. Analysis was primarily carried out using FAMIAS (Zima 2008), an interactive package in which the user guides each step of the frequency analysis process. A minimum signal-to-ratio (SNR) of four was used with FAMIAS to determine if an extracted frequency was statistically significant. Frequency analysis was also carried out using SigSpec (Reegen 2011), which uses the spectral significance rather than the signal-to-noise ratio as the statistical quantity to determine if a frequency is significant. Details of the spectral significance can be found in Reegen (2007). Briefly, the significance spectrum is based on an analytical solution of the probability that a discrete Fourier transform (DFT) peak of a given amplitude does not arise from white noise in a non-equally spaced data set which is typical of astronomical light curves. The underlying Probability Density Function (PDF) of the amplitude spectrum generated by white noise can be derived explicitly if both frequency and phase are incorporated into the solution. The spectral significance depends on frequency, amplitude, and phase in the DFT, and takes into account the time-domain sampling. Reegen (2007) states that the spectral significance is an unbiased statistical estimator.

SigSpec operates in a batch processing mode. The user provides a file of data and sets analysis options in an initialization file. SigSpec then reads both files and proceeds to analyze the data without further input from the user. A minimum spectral significance of five was used with SigSpec to determine if a frequency was statistically significant. This is equivalent to an SNR of four used with FAMIAS.

The package Period04 (Lenz and Breger 2005) Version 1.2 was also used, primarily as a check on the frequencies reported by FAMIAS. Period04 is an interactive package in which the user guides each step of the analysis. The frequencies and amplitudes reported by Period04 were sufficiently close to those of FAMIAS that the results obtained from Period04 are not reported separately. For example, in the Sector 12 data the first 25 identified frequencies where the same for Period04 and FAMIAS.

Recently Rea (2022a, b) proposed a simple modification to the method of frequency analysis which involved breaking up the frequency range to be analyzed into non-overlapping ranges and particularly suited frequency analysis software which used batch processing such as SigSpec. The method of splitting the frequency range was subjective and based on a visual inspection of the grouping of frequencies in the periodogram. The periodogram in Figure 2 did not have particularly clear gaps in the manner of either Rea (2022a) Figure 6 or Rea (2022b) Figure 4. Nevertheless, we split the full range into six sub-ranges in two different ways. Table 4 gives the ranges; the results part of the Table will be discussed further below. The reasoning is as follows and one possible alternative is also given:

Table 2. Details of the TESS data used in this paper.

Sector	*JD Range*	*Days of Observations*	*Usable Data Points*	*Amplitude (Mag.)*
12	1624.96–1652.89	27.93	19,086	0.0531
27	2036.28–2059.77	23.49	16,156	0.0525
39	2361.77–2389.72	27.95	19,337	0.0547

Notes: The JD Range gives the observation dates as Barycentric Julian Date –2457000. The final column reports the maximum amplitude of the light curve during the sector.

Table 3. A summary of the significant frequencies reported by FAMIAS (SNR > 4) and SigSpec (significance > 5).

	FAMIAS			*SigSpec (0–50)*		
Sector	*DScuti*	*GDor*	*Other*	*DScuti*	*GDor*	*Other*
12	20	0	0	483	45	6
27	24	3	0	368	41	5
39	26	2	0	460	47	7
				SigSpec (0–25)		
12	—	—	—	380	45	7
27	—	—	—	312	40	4
39	—	—	—	375	46	7

Notes: The frequency range used for γ Dor (GDor) was 0.3 to 3 cycles d^{-1}, for δ Scuti (DScuti) > 3 cycles d^{-1}; frequencies outside these ranges were classified as "other." The first set of results for SigSpec covers the frequency range 0 to 50 cycles d^{-1}, and the second set covers the range 0 to 25 cycles d^{-1}.

Table 4. The numbers of significant frequencies reported in the two restricted range analyses using SigSpec.

Range	*Sector 12*	*Sector 27*	*Sector 39*
0–3	0	3	0
3–7	0	0	0
7–9.5	6	9	4
9.5–11.1	25	23	19
11.1–16	72	54	69
16–50	40	32	33
Total	143	121	125
11.1–12.5	20	23	23
12.5–50	90	62	80
Total	141	120	126

0–3 This range included the γ Dor frequencies and lower. An alternative would have been to extend this range to a frequency of around four cycles d^{-1} because there were a number of low peaks in the periodogram, one of which is the frequency G1 of Table 6, above the three cycles d^{-1} cutoff.

3–7 This frequency range appears devoid of any peaks in the periodogram apart from the G1 frequency just mentioned.

7–9.5 There is a very small gap in the periodogram at around 9.5 cycles d^{-1} where there are no distinct peaks visible.

9.5–11.1 In common with the previous frequency range there is a very small gap in the periodogram at around 11.1 cycles d^{-1} where there are no distinct peaks visible.

11.1–16 This frequency range was sparsely populated with frequency peaks with the last visually important peak just inside the cut-off frequency.

16–50 The final frequency range had no visually important peaks. We also ran an analysis on the range 16–25 cycles d^{-1} but this gave identical numbers of frequencies as the longer (to 50 cycles d^{-1}) range and are not reported separately.

A second restricted range analysis was run splitting the range 11.1–50 cycles d^{-1} as follows:

11.1–12.5 This split took advantage of a clear region of very low peaks in the periodogram around 12.5 cycles d^{-1}.

12.5–50 Given the spacing between the visually important peaks above 12.5 cycles d^{-1} the final group of frequencies was analyzed as a single group. We also ran an analysis of the 12.5–25 cycles d^{-1} range but these gave identical numbers of frequencies as the longer (to 50 cycles d^{-1}) range and are not reported separately.

User-written R Code (R Core Team 2019) was used to prepare the data, plot the light curves, and further analyze the output of FAMIAS, Period04, and SigSpec. An important task carried out in R was to check whether each statistically significant frequency matched a distinct feature in the periodogram or was a spurious frequency resulting from the pre-whitening process used by all three packages; see Balona (2014) for a study of these types of spurious frequencies.

3. Results

Figure 1 presents the full light curves for the three sectors' observations. The approximately one-day data gaps were caused by the data download from the satellite to the ground.

Figure 2 presents the periodograms of the data and of the residuals after all significant frequencies were fitted and removed. The lower panel presents the spectral window for the Sector 12 data as generated by FAMIAS. The periodograms and spectral windows for Sectors 27 and 39 were not sufficiently different from Sector 12 to warrant reporting them separately.

Initially, frequency analysis was carried out to 100 cycles d^{-1} because Bedding *et al.* (2020) had reported statistically significant frequencies in some δ Sct stars up to 80 cycles d^{-1}. The periodogram for the σ Oct was featureless beyond 22 cycles d^{-1} for all three sectors' data and so subsequent analysis was reduced to cover the frequency range 0 to 25 cycles d^{-1}.

The default frequency range for SigSpec is 0 to 50 cycles d^{-1} and this was initially run. Because of the featureless periodogram above 25 cycles d^{-1}, a second set of analyses was run using the range of 0 to 25 cycles d^{-1}. Both sets of results are reported here in Table 3.

A summary of the results of the frequency analyses by FAMIAS and SigSpec are presented in Table 3. The frequency ranges for δ Sct, γ Dor were guided by Catelan and Smith (2015) Table 9.1. 0.3–3 cycles d^{-1} were classified as γ Dor frequencies; frequencies above three cycles d^{-1} were classified as δ Sct. Frequencies below 0.3 cycles d^{-1} were classified as Other.

Table 4 reports the number of significant frequencies reported by SigSpec when the two restricted range analyses were carried out.

A total of 41 distinct significant frequencies were reported by FAMIAS from the three sectors of observations. Of these only 13 frequencies in the δ Sct range were statistically significant in all three sectors. Table 5 presents details of these 13 frequencies using their ordering from the Sector 12 data.

γ Dor frequencies were reported by FAMIAS; details of these frequencies are presented in Table 6. Included in this Table is the 3.55 cycles d^{-1} frequency, which is above the usual cut-off frequency for γ Dor and hence could have been classified as a δ Sct frequency and included in Table 5. However, one should note that Grigahcene *et al.* (2010), in their Figure 2, showed that for hybrid γ Dor/δ Sct stars the γ Dor and δ Sct frequency ranges should not overlap. If we had taken their gap into account, which depends on a precise measure of the effective temperature, this particular frequency should perhaps be classified as Other.

Figure 3 presents a plot of the residuals after the 20 statistically significant frequencies identified by FAMIAS had been fitted to the Sector 12 data. Light curves of the residuals for Sectors 27 and 39 were also generated but are not reported separately.

4. Discussion

A feature of the light curves of all three sectors in Figure 1 was the extremely complex light curve which is typical of many δ Sct stars. Such complexity is the result of numerous pulsation frequencies being active in the star at the same time. Qualitatively, the light curve from Sector 39 does appear slightly different from the previous two Sectors in that the switching between high and low amplitude periods seems to be more frequent. When analyzed by FAMIAS there were more significant frequencies active in the Sector 39 data than Sector 12 (28 in Sector 39 and 20 in Sector 12), but the number of significant frequencies only differed by one between Sector 27 and Sector 39. A natural question which arises, particularly from the often abrupt changes in amplitude, which sometimes occur in a matter of only a few minutes, is whether this phenomenon is purely the result of numerous frequencies being active, or whether data exhibit some sort of deterministic chaos. When investigating the first option it was clear when fitting models to the data that even the inclusion of only the ten highest amplitude frequencies gave excellent fits and reproduced the often abrupt changes in amplitude well, meaning they were the result of beating between close frequencies. It can be seen in Table 5 that frequencies D3, D7, and D10 all had their highest amplitudes in the Sector 39 data. While there are empirical tests for chaotic behavior, such as those outlined in Sprott (2003), preliminary

Table 5. A summary of significant δ Sct frequencies.

	Frequency			*Amplitude*			
No.	*Sector 12*	*Sector 27*	*Sector 39*	*Sector 12*	*Sector 27*	*Sector 39*	*Crouzet et al. (2018)*
D1	10.49119	10.493168	10.492485	10.37	9.28	10.58	Y
	(68.984)	(67.383)	(99.237)	(0.69)	(0.67)	(0.58)	
D2	10.74000	10.740016	10.741156	3.09	3.23	3.18	Y
	(20.398)	(22.681)	(29.504)	(0.67)	(0.64)	(0.55)	
D3	9.35991	9.361072	9.361837	2.87	3.70	3.95	Y
	(19.996)	(26.882)	(43.653)	(0.67)	(0.64)	(0.55)	
D4	10.25491	10.252704	10.252759	2.80	2.76	2.78	Y
	(18.901)	(20.623)	(27.513)	(0.67)	(0.65)	(0.56)	
D5	11.42736	11.429488	11.429921	2.64	2.49	2.52	Y
	(16.922)	(18.187)	(19.914)	(0.67)	(0.64)	(0.55)	
D6	10.44644	10.43784	10.442393	1.95	1.81	1.99	Y
	(13.050)	(13.303)	(18.939)	(0.69)	(0.67)	(0.55)	
D7	9.71791	9.716448	9.719637	1.71	2.53	2.72	Y
	(11.940)	(18.568)	(29.584)	(0.69)	(0.66)	(0.58)	
D8	9.76803	9.769648	9.771518	1.49	1.42	1.52	Y
	(10.045)	(10.438)	(15.930)	(0.69)	(0.67)	(0.59)	
D9	9.13974	9.141888	9.140001	1.28	1.16	1.31	Y
	(9.185)	(8.342)	(14.046)	(0.67)	(0.64)	(0.55)	
D10	8.80680	8.795024	8.794724	1.11	2.13	3.06	Y
	(8.421)	(16.653)	(32.285)	(0.69)	(0.68)	(0.55)	
D11	10.91721	10.918768	10.914689	1.08	1.19	0.81	N
	(7.109)	(8.130)	(7.303)	(0.67)	(0.66)	(0.57)	
D12	11.75672	11.752944	11.755519	0.61	0.80	0.83	Y
	(4.334)	(5.533)	(6.659)	(0.67)	(0.64)	(0.55)	
D13	14.80867	14.823648	14.782507	0.48	0.41	0.39	N
	(4.541)	(4.372)	(4.410)	(0.67)	(0.64)	(0.57)	

Notes: Signal to noise (SNR) ratio is given in parentheses as reported by FAMIAS (Zima 2008) present in all three sectors of the TESS data. Amplitude is in millimagnitudes together with the the 3-σ confidence interval. Crouzet et al. *(2018) indicates whether the frequency was reported in their Tables B.1 or B.2.*

Table 6. The significant γ Dor frequencies from Sectors 12, 27, and 39 with the SNR below each frequency.

	Sector 12		*Sector 27*		*Sector 39*		
	Frequency	*Amplitude*	*Frequency*	*Amplitude*	*Frequency*	*Ampltiude*	*Crouzet*
No.	*(SNR)*	*(3sigma)*	*(SNR)*	*(3 σ)*	*(SNR)*	*(3 σ)*	*(2018)*
G1	3.547780	0.387	3.547376	0.392	3.545798	0.382	N
	(4.812)	(0.67)	(4.618)	(0.63)	(5.112)	(0.55)	
G2	—	—	0.697984	0.558	—	—	N
	—	—	(5.856)	(0.63)	—	—	
G3	—	—	2.845136	0.447	2.774739	0.438	Y
	—	—	(4.880)	(0.63)	(5.613)	(0.55)	
G4	—	—	0.614992	0.454	—	—	Y
	—	—	(4.831)	(0.64)	—	—	
G5	—	—	—	—	1.407943	0.440	N
	—	—	—	—	(4.219)	(0.55)	

Notes: The amplitude is in millimagniudes and the figure in brackets is the 3-σ uncertainty. The final column indicates whether the frequency was also reported in Crouzet et al. *(2018) Table B.1.*

analysis of the light curves and residuals showed no evidence of chaos. With the apparent adequacy of the models composed only of sinusoids, no further analysis of this type was carried out.

Table 5 presents details of the 13 δ Sct frequencies which were active in all three Sectors of the TESS data. As may be seen in the final column of the Table, 11 of these frequencies were also reported by Crouzet *et al.* (2018) in either their Table B.1 or B.2, indicating their stability over decadal time spans. The early estimates of the dominant photometric frequency reported by McInally and Austin (1978), Coates *et al.* (1981), and Tsvetkov (1982) give a somewhat lower frequency than either Crouzet *et al.* (2018) or the present analysis of the TESS data. Given the short time baselines and higher levels of observational uncertainties in these early papers, we cannot conclude that these were genuinely different frequencies.

The frequency 10.058734 which was reported in the Crouzet *et al.* (2018) Table B.2 was also present in the Sector 27 data with an amplitude of 0.8 mmag and in the Sector 39 data with an amplitude of 0.67 mmag. These amplitudes were similar to that in their 2011 season's data.

Of the 13 frequencies listed in Table 5 four underwent significant changes in amplitude at at least the 3-σ level.

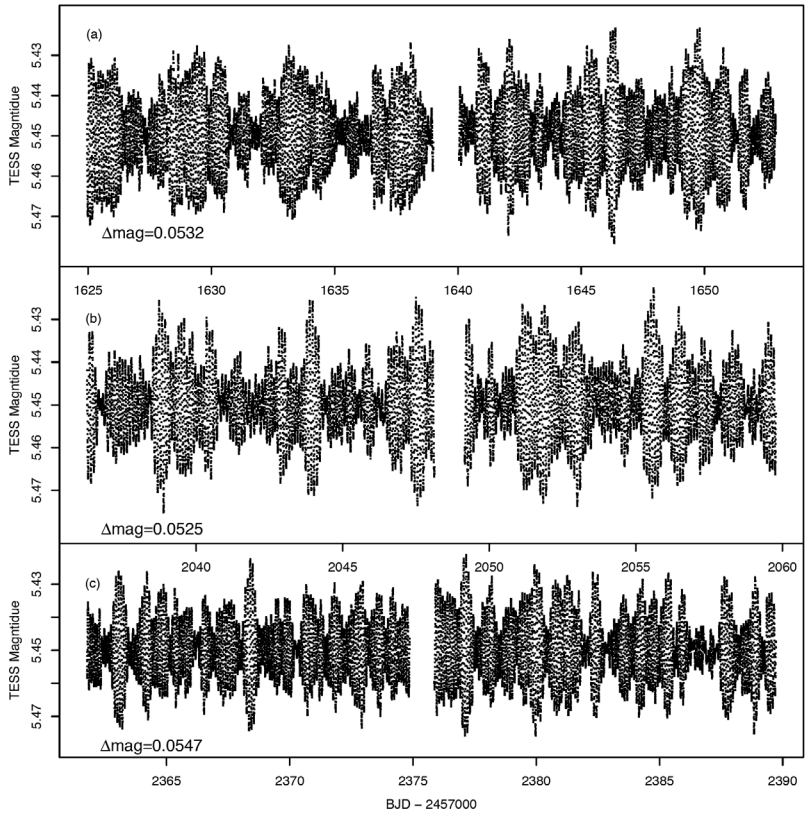

Figure 1. The full light curves for three sectors of TESS data for σ Oct/HD 177482. Panel (a) is Sector 12, panel (b) is Sector 27, and panel (c) is Sector 39. Δ mag is the range between highest and lowest magnitudes in that Sector's observations.

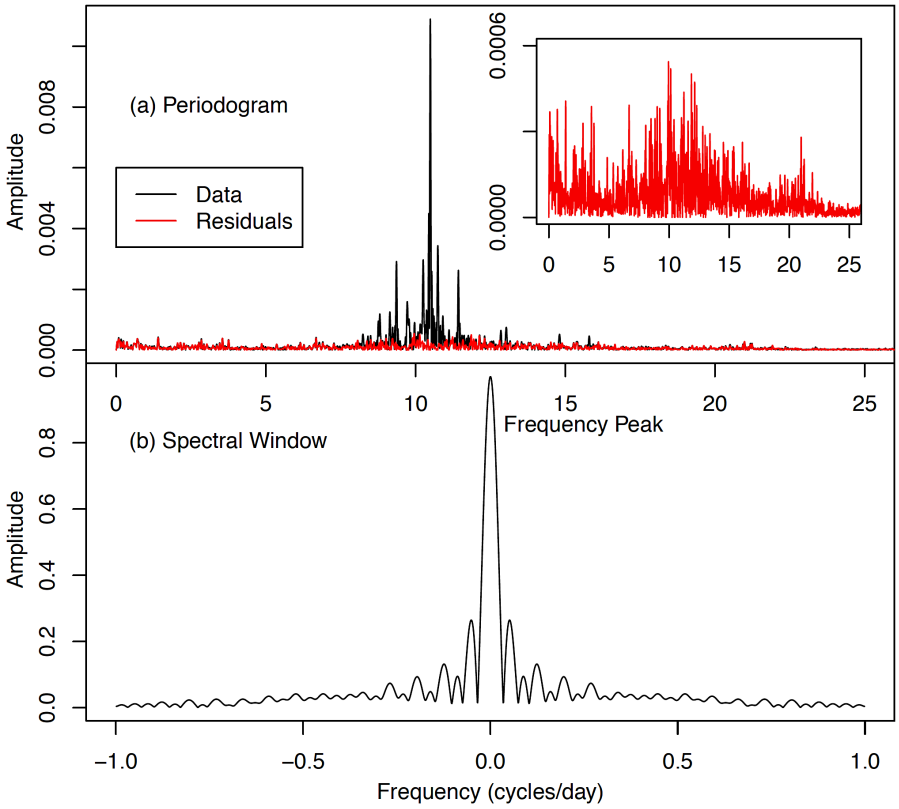

Figure 2. Panel (a) is the periodogram of the Sector 12 data in black while the red is the periodogram of the residuals after all the stiatistically signicant frequencies identied by FAMIAS were fitted. The inset graph in panel (a) is an expanded view of the periodogram of the residuals. Panel (b) is the spectral window from the same Sector.

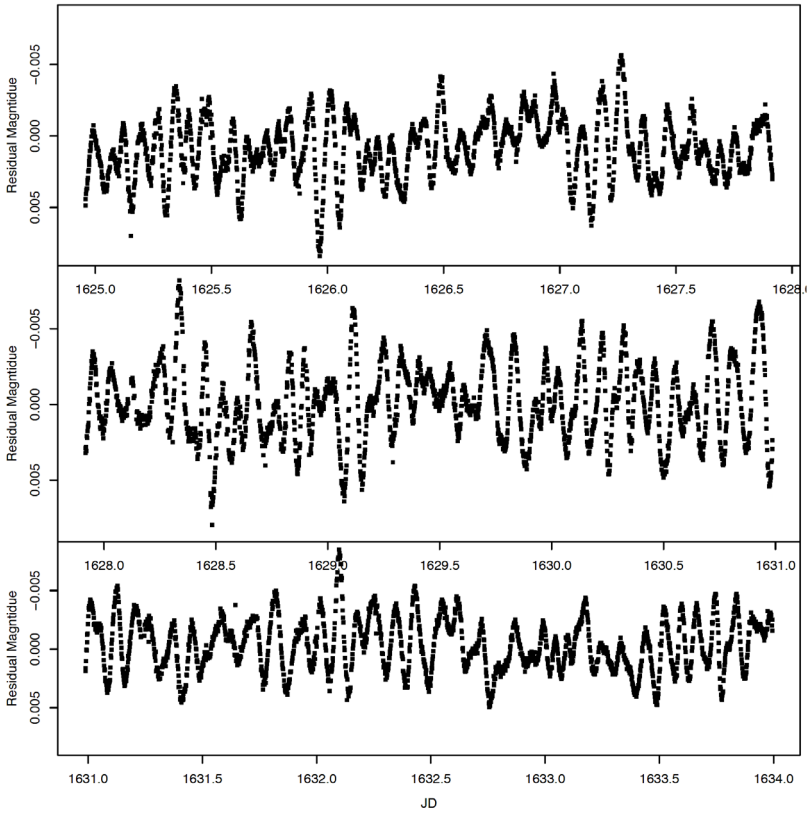

Figure 3. A plot of the residuals after all the statistically signicant frequencies were fitted to the Sector 12 data. The light curve covers an approximately nine day period rather than the full observing run in order to show the structure of the residuals more clearly.

They are frequencies D1 (10.49), D3 (9.36), D7 (9.72), and D10 (8.80). Each of these frequencies also underwent changes in amplitude in the Crouzet *et al.* (2018) data. Other frequencies were stable for both sets of data. For example, the amplitude of D2 (10.74) was stable across the four seasons of the Crouzet *et al.* (2018) data and the three Sectors of the TESS data. However, the amplitudes reported by Crouzet *et al.* (2018), about 2.77 mmag (amplitude for the combined data), were lower than each of the three TESS Sectors. To determine if this frequency undergoes amplitude modulation would require observations on a much longer time baseline than the approximately 27-day sectors of the TESS observation mode.

While frequency analysis was carried out using SigSpec (Reegen 2011), little is reported here because the presence of large numbers of spurious frequencies. For example, of the 483 δ Sct frequencies reported by SigSpec for the Sector 12 data, 138 of these were higher than 22 cycles d^{-1} and clearly did not correspond to any feature in the periodogram because the periodogram was featureless above this level. The first frequency reported in this featureless region was frequency number 179, meaning that the data had been through 178 cycles of prewhitening at this point in the analysis. As Balona (2014) pointed out, each cycle of prewhitening introduces a new frequency into the data, making it impossible to distinguish between real low amplitude frequencies and spurious frequencies. In fact, Balona (2014) writes: "Thus, it is not possible to count the number of individual modes with any degree of certainty below a certain amplitude level." As far as the author is aware, no statistical test has yet been implemented which can give guidance to the researcher that the "certain amplitude level" has been reached. This leaves anyone working on δ Sct stars in the unsatisfactory position where the decision on which frequencies to report as real and which to disregard as spurious is a subjective one.

Although restricted range analysis, reported in Table 4, did result in a useful reduction in the number of significant frequencies, there were still very large numbers of frequencies reported, the majority of which could not be identified with any feature in the relevant periodogram.

In the γ Dor range, active frequencies were reported in only two of the three sectors (see Table 6) with a maximum SNR of 5.86 which, qualitatively, is only weakly significant. While the 3.55 cycles d^{-1} frequency is included in this Table it is above the usual cutoff point for γ Dor frequencies so perhaps should be in Table 5. Only two of the remaining four frequencies were also reported by Crouzet *et al.* (2018) in their data. The 3-σ confidence interval was sufficiently large that it was not possible to analyze the data for amplitude modulation between sectors. The G3 frequency in the Table had a similar amplitude to that reported by Crouzet *et al.* (2018). While the G4 frequency appears to have a lower amplitude in the TESS data compared to the Crouzet *et al.* (2018) data, the large confidence interval made it impossible to reach a conclusion.

5. Conclusions

This analysis of the TESS data on σ Oct confirms Crouzet *et al.* (2018) that σ Oct pulsates in δ Sct mode but the evidence

for γ Dor pulsation modes as reported by them was weak in the TESS data. In two of the three Sectors' data a frequency in the γ Dor range exceeded an SNR of 5, with the maximum significance of 5.86. In the other Sector no γ Dor reached statistical significance, that is, no frequencies were reported with a SNR exceeding four.

The low amplitudes of the γ Dor frequencies made assessing whether they also undergo amplitude modulation difficult. The limited evidence suggests that they do because only two of the significant frequencies reported here were also reported by Crouzet *et al.* (2018), and two other γ Dor frequencies reported by Crouzet *et al.* (2018) were not detected in the TESS data. However, to resolve this question will require observations with longer time baselines than the approximately 27-days Sectors of the TESS mission.

The TESS data also confirm Crouzet *et al.* (2018) and, more generally, Bowman *et al.* (2016), that some of the δ Sct frequencies active in σ Oct undergo statistically significant amplitude modulation, including in the dominant 10.49 cycles d^{-1} frequency.

6. Acknowledgements

The author would like to thank NASA for making the data from its Transiting Exoplanet Search Satellite freely available and the TESS Asteroseismic Science Operations Center for operating their particular database (TASOC) of TESS photometry data.

The author would like to thank The American Association of Variable Star Observers for maintaining and making freely available the International Variable Star Index (VSX).

This research has made use of the SIMBAD database, operated at CDS, Strasbourg, France.

The author would like to thank an anonymous referee and editor Morrison for their constructive comments which helped improve the paper.

References

Balona, L. A. 2014, *Mon. Not. Roy. Astron. Soc.*, **439**, 3453.

Balona, L. A., Hearnshaw, J. B., Koen, C., Collier, A., Machi, I., Mkhosi, M., and Steenberg, C. 1994, *Mon. Not. Roy. Astron. Soc.*, **267**, 103.

Bedding, T. R., *et al.* 2020, *Nature* **581**, 147.

Bowman, D. M., Kurtz, D. W., Breger, M., Murphy, S. J., and Holdsworth, D. L. 2016, *Mon. Not. Roy. Astron. Soc.*, **460**, 1970.

Breger, M., and Beichbuchner, F. 1996, *Astron. Astrophys.*, **313**, 851.

Campbell, W. W., and Wright, W. H. 1900, *Astrophys. J.*, **12**, 254.

Catelan, M., and Smith, H. A. 2015, *Pulsating Stars*, Wiley-VCH, Berlin.

Centre de Donnees astronomiques de Strasbourg. 2007, SIMBAD Astronomical Database (http://simbad.u-strasbg.fr/simbad/).

Coates, D. W., Halprin, L., Moon, T. T., and Thompson, K. 1981, *Inf. Bull. Var. Stars*, No. 2047, 1.

Crouzet, N., *et al.* 2018, *Astron. Astrophys.*, **619A**, 116.

Eggen, O. 1956, *Publ. Astron. Soc. Pacific*, **68**, 238.

Gaia Collaboration. 2020, VizieR Online Data Catalog: Gaia EDR3 (Gaia Collaboration, 2020), VizieR On-line Data Catalog: I/350 (doi: 10.5270/esa-1ug).

Grigahcène, A., *et al.* 2010, *Astrophys. J., Lett.*, **713L**, 192.

Kafka, S. 2022, variable star observations from the AAVSO International Database (https://www.aavso.org/aavso-international-database-aid).

Krisciunas, K. 1993, *Bull. Amer. Astron. Soc.*, **25**, 1422.

Lenz, P., and Breger, M. 2005, *Commun. Asteroseismology*, **146**, 53.

McInally, C. J., and Austin, R. 1978, *Mon. Not. Roy. Astron. Soc.*, **184**, 885.

R Core Team. 2019, R: A Language and Environment for Statistical Computing, R Foundation for Statistical Computing, Vienna, Austria (https://www.R-project.org).

Rea, B. 2022a, *J. Amer. Assoc. Var. Star Obs.*, **50**, 8.

Rea, B. 2022b, *J. Amer. Assoc. Var. Star Obs.*, **50**, 107.

Rea, W. 2019, *Asteroseismology of HD 177482*, Technical Report, University of Canterbury, Department of Physical Sciences.

Reegen, P. 2007, *Astron. Astrophys.*, **467**, 1353.

Reegen, P. 2011, *Commun. Asteroseismology*, **163**, 3.

Ricker, G. R., *et al.* 2014, *Proc. SPIE, 9143*, id. 914320 (doi: 10.1117/12.2063489).

Sprott, J. C. 2003, *Choas and Time-Series Analysis*, Oxford Univ. Press, Oxford, UK.

TESS Asteroseismic Science Operations Center (TASOC). 2023, TESS Data for Asteroseismology (https://tasoc.dk/).

Tsvetkov, Ts. G. 1982, *Inf. Bull. Var. Stars*, No. 2084, 1.

Watson, C., Henden, A. A., and Price, C. A. 2014, AAVSO International Variable Star Index VSX (Watson+, 2006–2014; https://www.aavso.org/vsx).

Zima, W. 2008, *Commun. Asteroseismology*, **155**, 17.